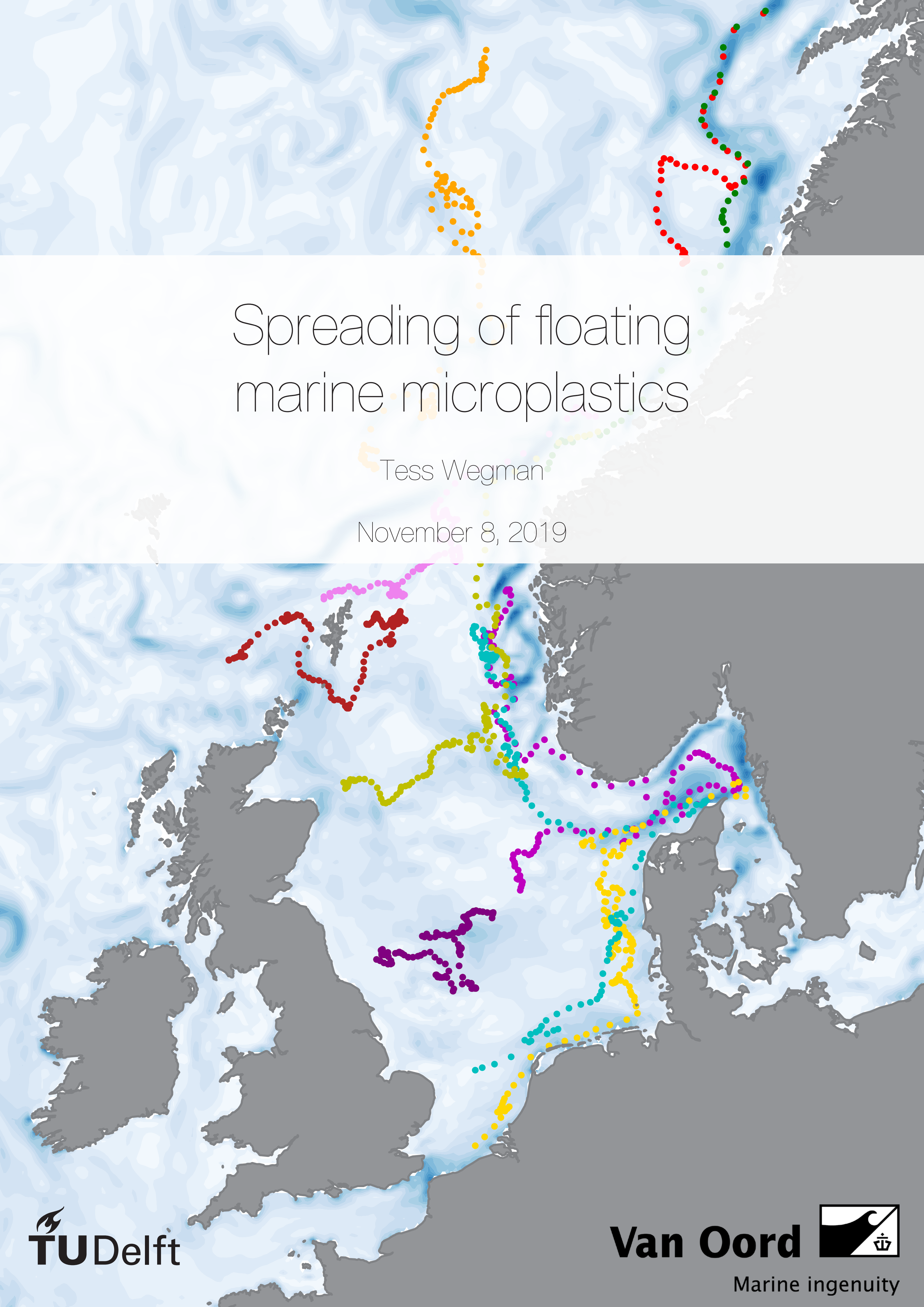

Spreading of floating marine microplastics

Tess Wegman

November 8, 2019

TU Delft

Van Oord
Marine ingenuity

Delft University of Technology

CIE4040 - Internship

Spreading of floating marine microplastics

By:
Tess Wegman
4350324

Supervisors:
Prof.dr. J.D. Pietrzak
Dr.ir. G.J. de Boer (Van Oord)
ir. L.M. Keyzer

Abstract

This study aims to get an insight into the particle trajectories that microplastics follow, after having been released in the North Sea.

For the computations daily-mean values of the surface currents are used, retrieved from the Mercator global ocean model. 2D particles trajectories are simulated for a year, with a 3rd party Python toolbox for Lagrangian simulation of particles: OceanParcels. Particles released from any location in the North Sea eventually get trapped in the Norwegian Coastal Current (NCC). From here they are being further advected to the North, at different moments in time for the particles released at different locations. The coastal processes in the NCC are mainly linked to wind and stratification, hence variations in flow patterns near the coast are linked to the seasons. When these flow pattern include large scale eddies, the particles follow a meandering and erratic path. Floating plastic particles released in the North Sea will flow northwards along the coast of Norway. Eventually those particles will end up in the Arctic region or get trapped in the Norwegian fjords, independently of the location of release. However, the time scale of the northward advection depends both on where the particle has been released and the environmental conditions.

Executive summary

During Offshore operations micro plastic particles may be released to the North Sea. This study aims to get an insight into the particle trajectories that these microplastics follow, after having been released in the North Sea. The released microplastics are assumed to be buoyant, and thus follow the currents at the sea surface.

Based on literature on the main surface flow patterns in the North Sea, the expectation is that plastic particles will circulate in the North Sea for several months to a year (depending on the location of release). Finally, they are most likely to get trapped in a strongly northward propagating current: the Norwegian Coastal Current (NCC). This current starts in the Skagerrak and runs along west coast of Norway to the Arctic region. Wind conditions and the time of the year cause fluctuations in the strength of this northwards propagating current. Usually the northward directed current velocity is weaker in spring and summer than in winter. These velocities are weakened by north-easterly winds, and further enhanced by south-westerly winds. The exchange of water between the fjord and the Norwegian Coastal Current is mainly governed by wind and the seasons.

The data for the flow field at the surface, sea surface salinity and sea surface temperature are obtained from the Mercator global ocean model (version NEMO 3.1), with a spatial resolution of 1/12°, which corresponds to roughly 8 km. Hence this model does not resolve coastal processes.

First a data analysis of surface currents, sea surface temperature and sea surface salinity is done for the NCC. This is compared to monthly-mean values of wind data obtained by satellite observations. The data has a spatial resolution of 1/4°.

Particle tracking of microplastics is done with OceanParcels, a 3rd party Python package for Lagrangian simulations. A simulation is run for one year, with input of daily-mean values of the ocean currents at the surface. This means the simulation for particle tracking is run in 2D mode. The coastal boundaries in the model are impermeable, which means that plastic particles cannot be washed ashore. Additional simulations with different hydrodynamic forcing is done: one with hourly-mean values of the ocean currents and one with the hourly-mean values of the total currents (total current = ocean current + tide-induced current + wave-induced current).

Data of 2018 of the NCC clearly shows that large scale eddies form along the coast of Norway after a freshwater outflow event from the Skagerrak. Very clear outflow events are observed several times in 2018. After these event, eddies are visible in both the sea surface salinity as well as the sea surface temperature. Also the vectors of the surface currents show eddying patterns. In constrast, the coastal current is northward directed parallel to the Norwegian coast in other cases. The wind patterns based on monthly-mean values for the wind speed and direction show a seasonal variation in line with literature.

Figure 1 shows particle paths of floating particles for eight different starting locations. Starting locations are indicated by a star with the size proportional to working depths of the works, and hence the amount of plastic. The coloured dots give an indication of the 'age' (in days) of the particle. Eventually all particles get trapped in the NCC, propagating northward.

Floating plastic particles released in the North Sea will flow northwards along the coast of Norway. Eventually those particles will end up in the Arctic region or get trapped in the Norwegian fjords. The final destination of the plastic particles does not depend on where they have been released. However, the time scale for how long it takes to be advected northwards

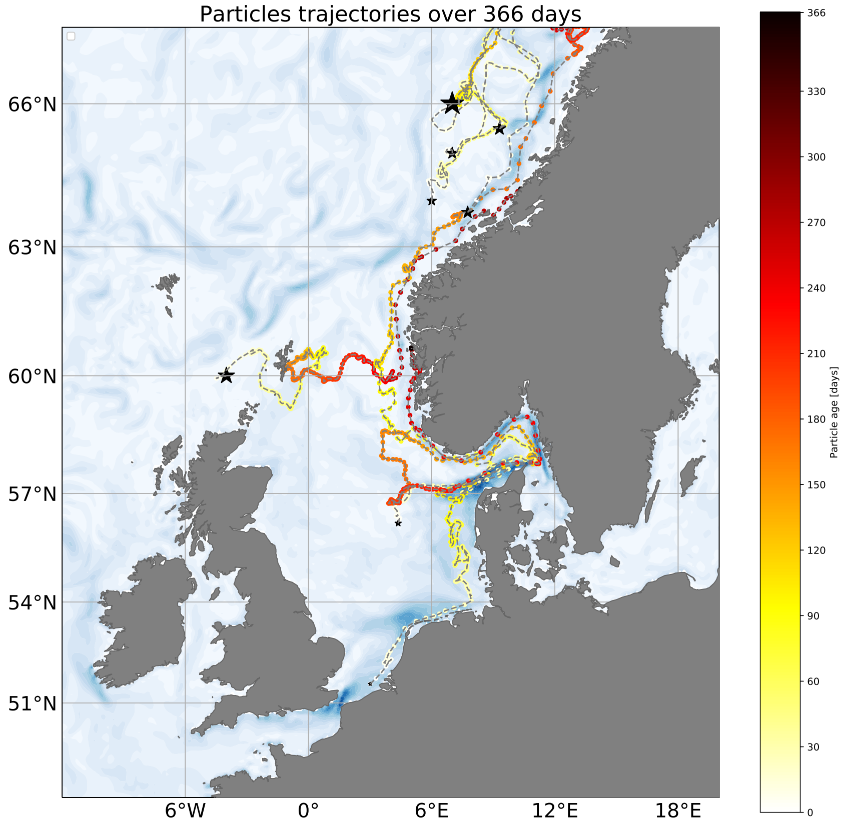

Figure 1: Particle trajectories for one year with daily mean input for the surface currents

depends both on where the particle has been released and the environmental conditions.

The computations have been done for 2D flows at the surface. From a study by Delandmeter and van Sebille, 2019 significant differences were found between 3D and 2D computations for the tracking of microplastics. The main differences in results is how much plastic is advected to the Arctic and how many particles get trapped along the coast of Norway. The model used is relatively coarse and cannot resolve coastal processes, understanding these dynamics is important to predict the behaviour of plastic particles near coastal boundaries. Particle trajectories for individual particles released from the same positions with both daily-mean values and hourly-mean data of the flow field, showed a clear difference. The importance of temporal resolution could be further looked into for future studies. As well as considering more 3D effects and coastal processes.

Table of Contents

1 Introduction

1.1 Problem statement

The Offshore operations at the North Sea and Norwegian Sea typically take place at offshore wind turbines, as well as oil and gas fields, at subsea structures, pipelines and cables on the seafloor (Van Oord, 2019a). There is a negative side effect to these offshore operations During Offshore operations microplastic particles may be released into the North Sea and as soon as microplastics enter the environment, it is practically impossible to remove them again. Marine plastics and especially microplastics are harmful for marine life.

1.2 Objective

Van Oord aims for sustainability, which can be seen in the Sustainable Earth Actions (S.E.A.) programme (Van Oord, 2019b). Van Oord has acknowledged this problem of the plastics released through the offshore operations and has an objective to tackle this problem. Van Oord applies the general multi-layer approach as for all environmental issues: first avoid, then minimise, mitigate and finally compensate. A previous study assessed the amount of plastic released. This 2 months study is a continuation of that study and aims to get an insight into the paths that these plastics might have followed after being released in the North Sea.

The main objective is to get a preliminary insight in the plastic particle paths and writing a recommendation in how to further tackle this problem. For this the the following research question will be answered: *How will microplastics spread in the North Sea after they have been released during offshore operations?*

With the following subquestions:

- *What are the general current patterns in the North Sea;*
- *What physical processes might influence plastic particles?*
- *Where do buoyant particles end up when released at the surface?*

1.3 Approach

The Lagrangian simulator, OceanParcels, will be used to track buoyant microplastic particles in the North Sea. For the input of the flow field, surface currents from the Mercator global ocean model are used.

1.4 Outline

Chapter 2 generically describes marine plastics, placing the problem in a more general context. Secondly, a brief summary of literature study providing an insight in the flow patterns in the North Sea and processes influencing the NCC is given in Chapter 3 and Chapter 4. Based on this a rough prediction will be made where the microplastics will go. Chapter 5 describes the approach of the computational analysis. Chapter 6 discusses the results after which conclusions are drawn in Chapter 8 and finally a discussion of the implications is given in Chapter 7.

2 Marine plastic

'More than 5 Trillion Plastic Pieces Weighing over 250,000 Tons Afloat at Sea' (Eriksen et al., 2014). The low production costs in combination with a high durability make plastics a popular material in a wide variety of applications. Significant amounts of plastic enter the marine environment through rivers, waste at the beach and littering at sea (Lebreton et al., 2017). These amounts of (micro)plastic in ecosystems are of growing international concern, due to the adverse effects it has on the environment.

2.1 What are microplastics?

Plastic pieces which are smaller than 5 mm in diameter are called microplastics. Some plastics already have a size smaller than 5 mm just after production. For instance microbeads, which are being used as an ingredient of numerous beauty products. Other microplastics are formed by degradation of bigger pieces of plastic waste material (NOAA, 2018).

2.2 Negative environmental effects

The presence of microplastics in the marine environment causes several problems. First of all ingestion by marine species can occur. This has been observed in amongst other fish, oysters, shrimp, sea birds (Barboza, Vethaak, Lavorante, Lundebye, and Guilhermino, 2018) and zooplankton (Cole et al., 2013). Besides direct ingestion, animals higher in the food chain can also ingest microplastics by eating other species containing plastics (Barboza et al., 2018). This can cause an accumulation of plastics higher in the food chain. These facts also give rise to concern about human food safety. Microplastics have been found in different food products, and also in drinking water. Most microplastics leave the human body without being taken up. However, the impact of plastic in the food chain on human health is still unknown (NOS, 2019).
Microplastics contain additives, which can be toxic chemicals (Andrady and Rajapakse, 2019). Another negative effect of microplastics in the ocean, is that contaminants can adhere to the particles and accumulate over time. These plastic particles with toxic chemicals or accumulated contaminants such as pathogens are a potential threat to health of marine life and allow for those pathogens to spread more rapidly (Barboza et al., 2018).

2.3 Plastics released

The main fraction of released particles are microplastics, ranging from 0.5 mm to 4 mm in size. The macro plastics are mainly brittle and are expected to wear down to microplastics relatively quickly. The particles are estimated to be neutral buoyant, 50% plastic and 50% voids (Pot, 2019).

3 Current patterns North Sea

This chapter provides an insight into the circulation patterns in the North Sea. It describes the major currents and outlines the most important driving forces for those currents. This will help the understanding of how plastic particles will be advected once released in the North Sea.

3.1 General water mass circulation in the North Sea

The North Sea is a shelf sea located between the countries of the Netherlands, Belgium, France, Great Britain, Norway, Sweden and Denmark. In the north it is connected to the Atlantic Ocean and the Norwegian Sea. In the east it has a connection with the brackish Baltic Sea through four basins (the Skagerrak, the Kattegat, the Öresund and the Belt Sea) (Gustafsson, 1997). In the south it is connected to the Channel, where Atlantic water masses can enter as well (Beg, 2013).

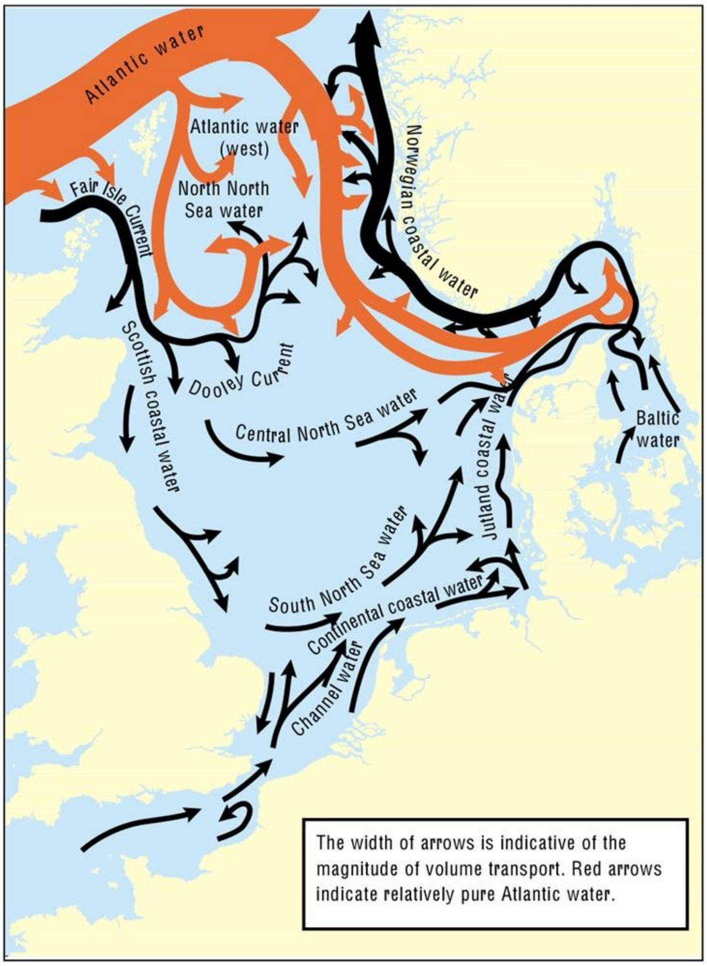

Figure 3.1: Schematic diagram of general water circulation of North Sea (OSPAR, 2000)

Figure 3.1 shows the main current patterns in the North Sea. The North Atlantic Current (NAC) brings saline and warm water from the tropical zones towards the North Sea (Pietrzak, 2018a). This mainly enters the North Sea between Scotland and Norway. The water that enters through the gap of the Fair Iles, is the Fair Isle Current. Some Atlantic water can also enter through the Channel, however this inflow it less than 10% (OSPAR, 2000). Off the coast of

Norway the NAC splits into a northward propagating branch and the currents flowing towards the North Sea. The Norwegian trench is located west of Norway is very deep, hence there is a strong northward current in the trench: the Norwegian Coastal Current (NCC). The NCC originates from North Sea water, Baltic water and Atlantic water that mixes in the Skagerrak.

A general anti-clockwise (cyclonic) circulation can be observed around the continental edges. This motion is the same direction as the Kelvin wave propagating the the North Sea (Holt and Proctor, 2008).

3.2 Driving forces of the currents in the North Sea

Currents in the North Sea are forced by different components listed below: (Holt and Proctor, 2008)

- tidal forcing;
- density gradients;
- wind forcing;
- oceanic sea level (pressure) variation.

3.2.1 Tidal flow

In the North Sea there is a generally anti-clockwise propagating Kelvin wave. The North Sea has a mainly semi-diurnal tide, with dominant components M2 and S2. The Kelvin wave enters the North Sea at the northern connection with the Atlantic and first propagates south along the coast of England and then around the amphidromic points and then propagates further northwards along the Dutch and Danish coast (Bosboom and Stive, 2015). In principle the tide is a backward and forward moving wave, hence in theory no net mass transport over a tidal cycle. However, asymmetry in the tidal signal cause residual tidal currents in the North Sea.

3.2.2 Stratification

Stratification mainly occurs due to river inflow from the continents and brackish water of the Baltic Sea. Other sources of stratification are saline (and warm) water from the Atlantic Ocean, which enters through the NAC, and solar radiation. Destratifying mechanisms are the tides, wind and waves.

In winter the North Sea is mainly well-mixed, with exception for the Skagerrak, Kattegat and Norwegian trench (OSPAR, 2000). In summer and autumn the stratification is most relevant for driving the flows. This causes the density driven currents to be highly variable in magnitude throughout the year (Holt and Proctor, 2008).

The Rhine ROFI is depicted in Figure 3.1 as 'Continental coastal water' and flows from the coast of the Netherlands all the way to the North along the coasts of the Netherlands and Denmark, partially Sweden and Norway (Pietrzak, 2018a). In the Skagerrak this continental coastal water mixes with Baltic water and Atlantic water.

The Baltic Sea is connected to the much saltier North Sea through the Skagerrak and series of deep basins. Due to this major density difference the connection between the North Sea and the Baltic Sea is similar to estuarine circulation (Pietrzak, 2018b). This and the topography of deep and narrow trenches restrict the water exchange between the two seas (Gustafsson, 1997). Most of the water that enters the Skagerrak moves in a cyclonic way back to join the NCC (Maslowski and Walczowski, 2002).

3.2.3 Atmospheric pressure variation

Atmospheric pressure variations can drive changes in the oceanic sea level. This barotropic forcing can drive flows (Pietrzak, 2018a). In the North Sea the North Sea Oscillation (NAO) index is defined, which is the pressure difference between Lisbon and Iceland. The NOA index is closely related to the westerly winds. Strong westerly winds correspond to a high NAO index and large transport values (Winther and Johannessen, 2006).

3.3 Prediction of particle trajectories in the North Sea

The main driving forces of residual currents in the North Sea are stratification, sea level pressure variation, wind forcing and tidal forcing (Holt and Proctor, 2008). The general circulation pattern is cyclonic. The major inflow is at the north by inflow of Atlantic water, and the main outflow is in northern direction along the Norwegian coast through the NCC.

Depending on where particles have been released, they are expected to undergo different trajectories. For this study the assumption is made that the plastic particles are buoyant (see Section 2.3) and thus follow the surface currents.

Based on the major flow patterns in the North Sea and the fact that the particles are buoyant, the expectation is that most of the particles will eventually end up in the NCC and be advected north along the coast of Norway. From here different scenarios can be expected for buoyant particles released in the North Sea:

- getting trapped in the Norwegian fjords;
- being advected to the Arctic region.

4 Processes influencing the Norwegian Coastal Current

Once plastic particles have reached the Norwegian Coastal Current (NCC), coastal processes in and near the NCC might have a great influence of whether plastic particles will flow towards the fjords or whether they will be further advected to the Arctic region. The NCC is a current west of the coast of Norway. As can be seen in Figure 3.1 it originates in the Skagerrak and is characterised by strong northwards directed surface currents. The average magnitude of the current is estimated 0.50 m/s, but regularly exceeds 1.0 m/s (McClimans and Nilsen, 1983) On the western side a front can be found between the NCC and the North Atlantic Current (NAC).

Bathymetry is an important factor of the main flow pattern of the NCC (Ersdal, 2001). The dynamics are mainly influenced by changing fresh water fluxes and wind forcing (Mork, 1981). This chapter will further explain these key physical processes influencing the flow patterns of the NCC.

4.1 Topographic steering

Topographic steering is the phenomenon where a current follows the path with a constant potential vorticity: $\frac{(\zeta+f)}{H}$. With f the planetary vorticity, ζ relative vorticity (rotation of the fluid) and H the water depth. If $f \gg \zeta$ Topographic steering can be described by Equation 4.1 (Pietrzak, 2018a):

$$u\frac{\partial}{\partial x}\left(\frac{f}{H}\right) + v\frac{\partial}{\partial y}\left(\frac{f}{H}\right) = 0 \quad \rightarrow \quad \frac{f}{H} = constant \tag{4.1}$$

Consequently, flows are likely to follow depth contours. The NCC follows the bathymetry of the Norwegian Trench, which has depths up till 730 m (Britannica, n.d.). It runs from the Skagerrak northwards along the coast of Norway. Close to the Norwegian coast it reaches to depths over 100 m (NHL Sintef-Gruppen, n.d.), and further offshore it is located mainly at the surface, see yellow area in Figure 4.1a. Topographic steering causes the northward moving NAC current to partially branch off southward, around the Tampen Banks. At location of the Tampen Banks the depth H decreases, according to Equation 4.1 the Coriolis parameter f should also decrease, which implies a southward motion. This southward directed branch, at the western slope of the Norwegian Trench, feeds the North Sea, as discussed in Section 3.1. The NAC is depicted with pink in Figure 4.1a.

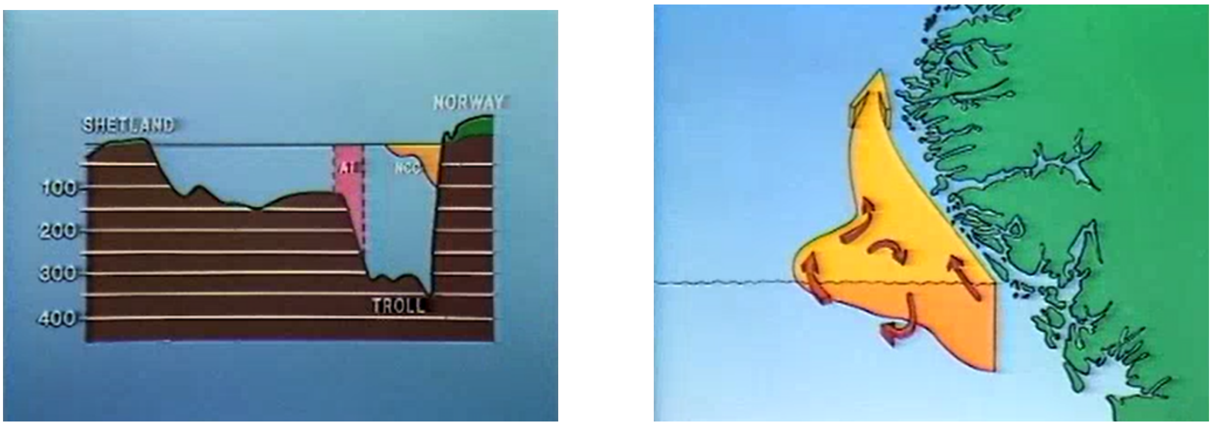

(a) (b)

Figure 4.1: (a) cross-section of the Norwegian trench showing the NCC (yellow) and the NAC (pink) (b) formation of eddies in the NCC (NHL Sintef-Gruppen, n.d. on behalf of T.A. McClimans)

.

4.2 Stratification

The freshwater sources of the NCC are brakisch water from the Baltic (50%), fresh water runoff from the Norwegian coast (40%), and freshwater runoff from the North Sea (10%) (van Miltenburg, 2017). The NCC has a front with the more saline NAC on the west. Table 4.1 gives the temperatures and salinities of water masses mentioned above.

Water mass	Salinity [PSU]	Temperature [°C]
Baltic water	8.8-20	0-20
Norwegian coastal water	32-34.5	3-18
Continental coastal water	31-34	0-20
Atlantic water	>35	7-15

Table 4.1: Salinities and temperatures of water masses (OSPAR, 2000)

4.2.1 Estuarine circulation

Figure 4.2 shows the water masses and some physical processes mainly found in fjords. A sill is located at boundary between the fjord and the sea. The line indicated with $\rho(z)$ represents the pycnocline. The surface water, consisting of fresh river runoff, has a lower salinity than the intermediary water in the fjord basin. Between these water masses an estuarine circulation can be found: offshore directed flows at the surface and onshore directed flows at intermediate depth. (Stigebrandt, 2012). The currents speeds of those density driven flows are usually 0.01-0.2 m/s (Inall and Gillibrand, 2010). The freshwater runoff is mainly due to melting ice, which is biggest in spring and summer.

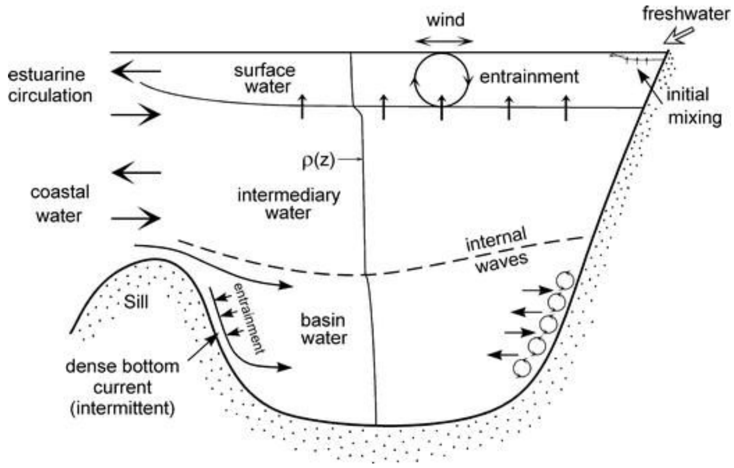

Figure 4.2: Water masses and some physical processes and modes of circulation in fjords (Stigebrandt, 2012)

4.2.2 Formation of eddies

Baroclinic instabilities at the front between the NCC and NAC can generate large eddies. The location of those eddies are on the western side of the NCC, as can be seen in Figure 4.1b. These eddies can grow till diameters of 50-100 km, and local currents speeds up to 1 m/s have been reported (McClimans and Nilsen, 1983). The occurrence of these large eddy structures are associated with large outflow events of the Baltic water into the NCC (Ersdal, 2001). These outflow events usually occur between February and August.

4.3 Coriolis

The effect of the Earth rotation on flows is often defined as the Coriolis force. The internal Rossby radius of deformation R_I is the length scale from which Coriolis plays a role in stratified flows, and is given by Equation 4.2. With g' the reduced gravity, given by Equation 4.3 and f the Coriolis parameter, given by Equation 4.4 (Pietrzak, 2018a). R_I has typical values of 2–5 km on the North Sea shelf and 14 km in the Norwegian Trench according to Holt and Proctor, 2008.

$$R_I = \frac{\sqrt{g'H}}{f} \tag{4.2}$$

$$g' = \frac{\rho_1 - \rho_2}{\rho_0} g \tag{4.3}$$

$$f = 2\Omega sin(\varphi) \tag{4.4}$$

For fjords with a width significantly smaller than R_I, the effect of Coriolis is negligible. In this case the fjord can be schematised as a 2D case. For fjords with a large width compared to R_I, fronts and resulting instabilities can form in lateral direction. (Farmer and Freeland, 1983)

4.4 Wind forcing

Wind forcing on the sea surface can generate a friction induced mass transport perpendicular to the wind direction: Ekman mass transport. This transport is to the right in the Northern hemisphere.

Wind shear stress at the sea surface induces a surface flow at an angle of 45° to the right, see Figure 4.3. This flow induces a shear stress at the water layer below at an angle smaller than 45° to the right, generating another flow with a smaller velocity than the surface flow. This goes on up till the bottom of the Ekman layer (D_E), where the flow vector is oppositely directed to the wind direction and close to a magnitude of zero. The full patterns of these flow vectors forms a spiral, as depicted in Figure 4.3. When integrating all these flow velocities (u_E) over depth ($-2D_E$ to η), this gives the total Ekman mass transport according to Equation 4.5, with water density ρ_0 (Pietrzak, 2018a).

$$M_{xE} = \int_{-2D_E}^{\eta} \rho_0 u_E dz \tag{4.5}$$

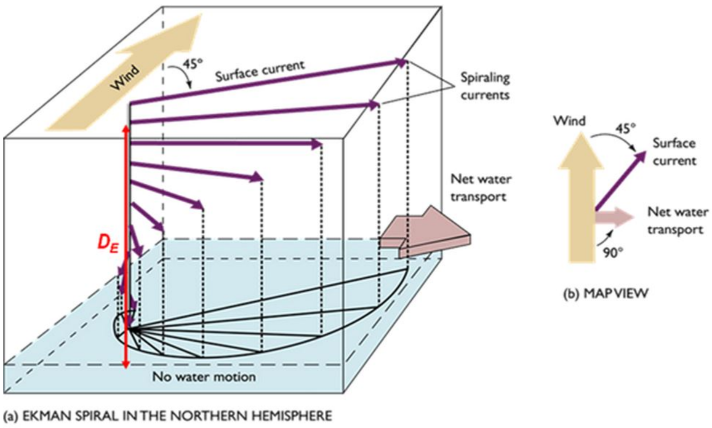

Figure 4.3: Ekman spiral and Ekman mass transport (OffshoreEngineering.com, n.d.)

4.4.1 Skagerrak outflow

The Skagerrak is highly sensitive to wind-induced Ekman transport. This causes the exchange conditions to alternate between blocking and large outflowing events. (Partial) blocking occurs under conditions of strong south-westerly winds, in this case the flow is directed towards the Skagerrak. When the wind direction changes, outflow is allowed again. This outflow is further increased with north-easterly winds. An additional effect of north-easterly winds is the drop in sea level in the Kattegat results in outflow from the Baltic sea, and subsequently a northward Ekman flow in the Kattegat, implying Skagerrak outflow. The reverse effect is observed with south-westerly winds (Gustafsson, 1997).

4.4.2 Upwelling and downwelling

Close to a coastal boundary, Ekman transport can result in up- or downwelling. Coastal up- or downwelling occurs to satisfy continuity in the water balance (Pietrzak, 2018a).
To illustrate the effects we assume a narrow fjord with east-west orientation. Along the coast of Norway north-easterly winds induce offshore-directed Ekman mass transport and subsequently upwelling along the shelf. This results in fjordic inflow at low and intermediate layers, and outflow at the surface layer, see upper section of Figure 4.4. These conditions are most common in spring and summer, and upwelling events are associated with smaller northwards flow velocities of the NCC (Skagseth, Slotte, Stenevik, and Nash, 2015). The opposite happens with south-westerly winds: onshore directed Ekman transport induces downwelling. There is

fjordic outflow at the lower layer, and to keep balance there is an inflow at intermediate depth. Depending on the magnitude of the wind and the amount of freshwater runoff, the outflow at top layer is either present (but reduced) or blocked. Downwelling causes stronger northward directed component of the NCC.

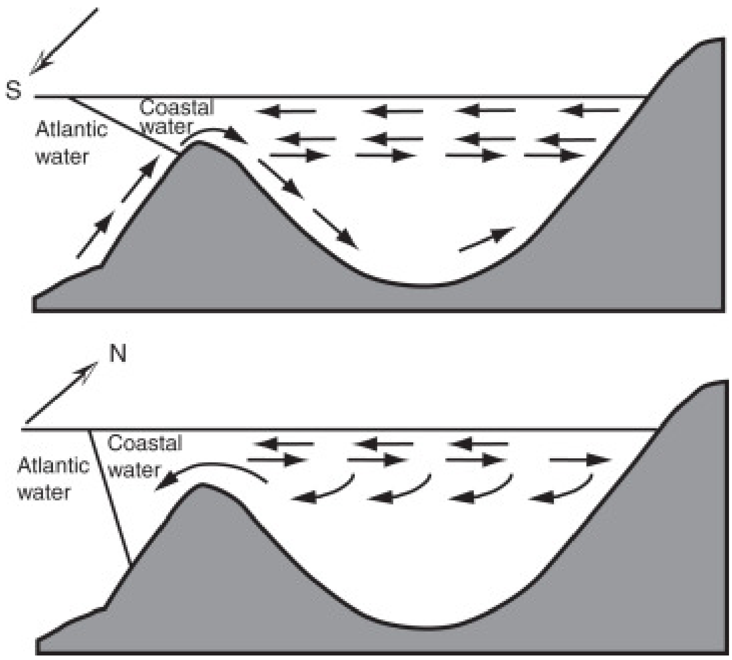

Figure 4.4: Flow patterns of wind-induced water exchanges between the coast and fjords with prevailing northerly wind (upper panel) with exchange of basin water, and southerly wind (lower panel) (Tande, 2001)

4.4.3 Wind set-up

Theoretically, an ageostrophic balance could be achieved in a narrow fjord (compared to the Rossby Radius) if cross-shore winds, aligned with the fjord axis, are present for a long enough time. According to Klinck, O'Brien, and Svendsen (1981), cross-shore wind only initiates a wind set-up, but does not result in a volume change in the fjords. This implies no net current flowing in and out the fjord due to wind set-up.

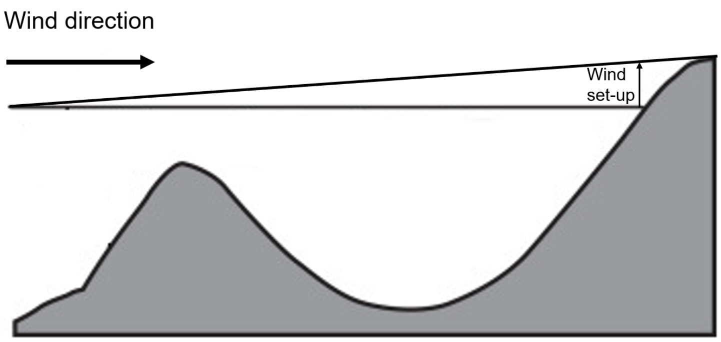

Figure 4.5: Wind set-up in a narrow fjord, if the wind direction is aligned with the fjord, an edited figure of Tande (2001)

4.5 Relation to particle paths

Plastic particles in the NCC have two main options; they can be advected northwards along the coast of Norway towards the Arctic or they can be advected eastward into the fjords.

The current patterns in the NCC are highly linked to seasonality. In spring and summer the expected chance is smallest that plastic particles get trapped into the fjords. In this season the estuarine circulation is strongest, which is characterised by an offshore directed surface current. Additionally, north-easterly winds are more prominent in spring and summer. Under this wind direction coastal upwelling occurs, which enhances offshore directed currents at the surface and at intermediate depth (upper panel Figure 4.4). In winter and autumn the wind direction is also more favourable for coastal downwelling (lower panel Figure 4.4). As explained in Section 4.4.2 the outflow at the surface is reduced or blocked, causing a higher change for particles to enter the fjord.

The north-easterly winds also cause freshwater outflow events from the Skagerrak, which result into whirls on the western side of the NCC. This delays the northward advection of the particles.

A qualitative estimate can be made for narrow fjords with an east-west orientation. This way a 2D configuration can be assumed. Under conditions of a weak river outflow from the Norwegian coast, in combination with south-westerly winds (coastal downwelling) the chance is highest that plastic particles flow into the fjords.

5 Methodology

The Lagrangian simulator, OceanParcels, is used to track floating microplastic particles in the North Sea. For the input of the flow field, surface currents from the Mercator global ocean model are used. First a data analysis of the NCC is done, to see whether the data of the Mercator model reproduces the general flow patterns found in literature.

5.1 Microplastics

However, the rock scraping off the plastic are of a much harder material, which makes it highly unlikely that rock particles will stay behind in the released plastic particles. Plastic particles without rock contamination are expected to stay afloat, even if the voids are filled with saltier water at depth.

5.2 Mercator model hydrodynamic forcing

To obtain the flow field the Mercator model version NEMO 3.1 is retrieved from Copernicus (Copernicus Marine environment monitoring service, 2019). This global ocean data has a spatial resolution of 1/12° (roughly 8 km) with a spherical mesh. The velocity field is interpolated from the original model and projected on a standard collocated A-grid (flow variables are defined at the same locations/full grid point. The model is updated daily with observations. The data can be downloaded with a temporal resolution of hourly-mean, daily-mean or monthly-mean values. The daily-mean data only includes the ocean current velocity in northward and eastward direction ($\boldsymbol{vo}(x, y)$). Hourly-mean data has the total velocity in both directions ($\boldsymbol{v}_{total}(x, y)$ given by Equation 5.1), consisting of the ocean current velocity ($\boldsymbol{vo}(x, y)$), tide-induced velocity ($\boldsymbol{v}_{tide}(x, y)$) and wave induced velocity, also named Stokes drift ($\boldsymbol{v}_{wave}(x, y)$). The computations use the daily-mean values of the ocean current ($\boldsymbol{vo}(x, y)$) at the surface.

$$\boldsymbol{v}_{total}(x, y) = \boldsymbol{vo}(x, y) + \boldsymbol{v}_{tide}(x, y) + \boldsymbol{v}_{wave}(x, y) \tag{5.1}$$

5.3 Lagrangian simulator for particle tracking

Particle tracking is done with a Python toolbox named Ocean**Parcels** ("**P**robably **A** **R**eally **C**omputationally **E**fficient **L**agrangian **S**imulator"). This package has been developed to track particles in combination with ocean models (OceanParcels project, 2019).

The grid used by OceanParcels v2.1 is based on the nodes at which the hydrodynamic values are defined. Each field is discretized on a structured grid that provides the node locations and instants at which the field values are given. It uses spherical mesh, but takes velocities in m/s. For the advection of particles a Runge-Kutta 4 scheme is implemented.

Computing particle trajectories with a Lagrangian method can be described with Equation 5.2 (Lange and van Sebille, 2017). Here $\boldsymbol{X}$ is the three-dimensional position of a particle, $\boldsymbol{v}(\boldsymbol{x}, t)$ is the three-dimensional velocity field at that location in the ocean model, and $\boldsymbol{X}_b(t)$ is a change in position due to 'behaviour' of the particle. This can be either a swimming fish or the sinking or uplifting of respectively heavy or buoyant particles.

$$\boldsymbol{X}(t + \Delta t) = \boldsymbol{X}(t) + \int_t^{t+\Delta t} \boldsymbol{v}(\boldsymbol{x}, \tau)\mathrm{d}\tau + \Delta \boldsymbol{X}_b(t) \tag{5.2}$$

5.4 Boundary conditions of the particle tracking simulation

The Mercator model has impermeable boundary conditions at the coastlines, which means that 'beaching' cannot occur. This is the input for the particle tracking simulation, where the impermeable coastlines are also implemented.

The boundaries of the domain for particle tracking are set as walls, as such that the particles that want to leave the domain stick at the boundary. This is for practical reasons, otherwise OceanParcels gives an error when a particle leaves the domain and then the calculation is ended.

5.5 Spatial and temporal scales

Time steps
Daily mean values of the eastward and northward ocean current velocities at the surface are used for the analysis. First of all daily-mean values of the hydrodynamic input are used. This means a Δt=24 h. A rule of thump is to take 1/10th of the hydrodynamic forcing time step as Lagrangian interpolation time step. So here simulations with a time step of Δt=3 h is used for the interpolation. No numerical stability analysis is done. However in Section 6.3 the chosen time step is validated.

Rossy Radius of deformation
R_I has typical values of 2–5 km on the North Sea shelf and 14 km in the Norwegian Trench (Holt and Proctor, 2008). Because the model has an 8 km resolution, this implies that eddies cannot be resolved, however for the Norwegian Coastal Current the large scale eddies, of order 50-100 km, can be shown.

Tidal period
As mentioned in Section 3.2.1, the North Sea has a semi-diurnal tide, hence the tidal period is roughly 12 hours. This means that in a computation with daily input for the flow field the 'back and forth' of the tide is not taken into account.

5.6 NCC

First a data analysis of the NCC is done. This is done to see whether the data of the Mercator model reproduces the general flow patterns found in literature.

Data of daily-mean values of flow velocities, sea surface salinity and temperature of the year 2018 are used. The data is retrieved from the Mercator global ocean model as described in Section 5.2. This is linked to the monthly-mean values of wind observation data from 2018 (only data till December is available).

For the analysis of wind patterns, data is retrieved from Copernicus. The used product is called 'Global Ocean Wind L4 Reprocessed Monthly Mean Observations'. From satellite observations, the monthly winds per grid point are estimated from a minimum of 25 values in the corresponding grid point. The spatial resolution is 1/4°. The data set is available up to and including November 2018, so data from January 2018 till November 2018 is used for the analysis.

5.7 Scenarios of particle tracking

The following cases will be considered, this is done for 8 particles released at locations according to Table 5.1. First a base case is considered, followed by some variations:

- Base case as supplied by Van Oord offshore operations: 1 year simulation with daily-mean values of the ocean currents;

- Different time scales for the Lagrangian time integration;
- Different time scale of the hydrodynamic forcing (hourly-mean);
- Different components of the hydrodynamic forcing (just ocean currents and total velocity including ocean current, tide-induced current and wave-induced current)

Particle nr	Location	Approximate working depth [m]
1	Southern North Sea	28
2	North Sea and Skagerrak	90
3, 4, 5, 6	Norwegian Sea	300
7	Shetlands	600
8	Barents Sea	1200

Table 5.1: Locations of released particles

6 Results

6.1 Data analysis NCC 2018

Figure 6.1 shows the surface ocean currents, sea surface salinity and sea surface temperature on the 3rd of January 2018. In January the salinities just off the coastal boundaries are about 35 PSU, which corresponds to a salinity of (the surface of) the Atlantic Ocean. The coastal waters have a density of 30 to 32 PSU, with higher salinities along the Norwegian border than along the Dutch and Danish coast. Relatively low temperatures are found in the entire region of the North Sea and Norwegian Sea, hence it is winter time. For the first half of January the currents just off the coast of Norway are directed parallel to the coast. The monthly mean wind (see Figure A.3a in Appendix A) is from south-westerly direction in the Skaggerak and in the North Sea. Along the coast of Norway, north of 63°N winds are north-westerly.

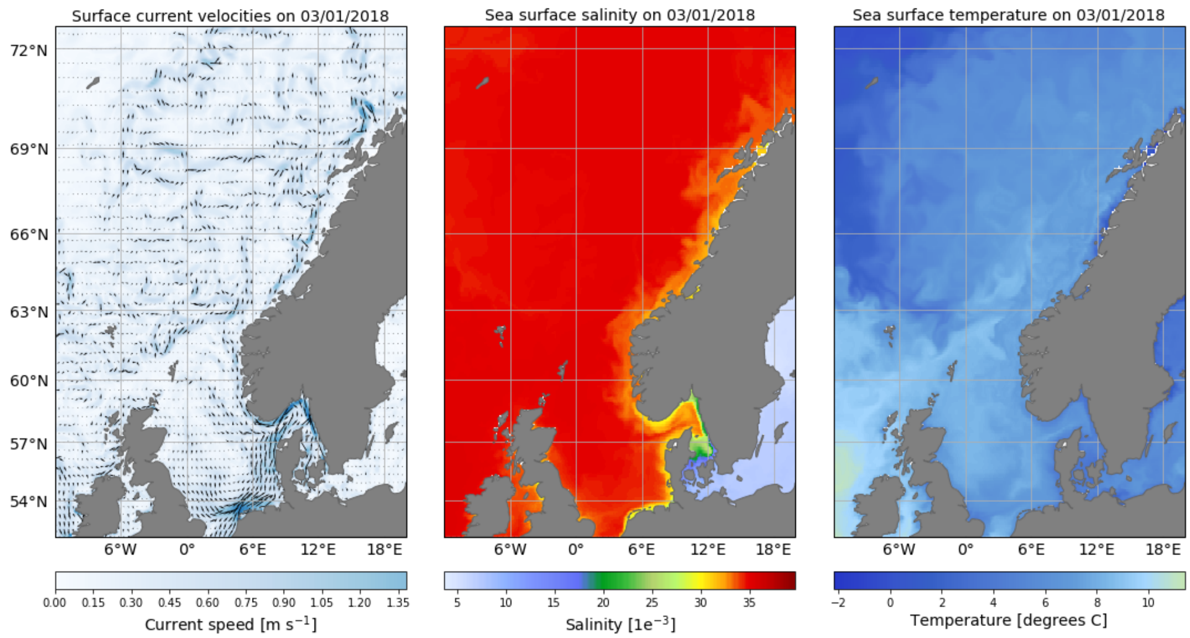

Figure 6.1: Surface currents, sea surface salinity and sea surface temperature for the North Sea and NCC on January 3rd 2018

Halfway January (see Figure A.1 in Appendix A) it looks like a small outflow event of the Skagerrak takes place. At the end of January small whirls are clearly seen in the surface salinity and along the Southern coast of Norway the velocities are not merely parallel to the coast anymore (see Figure A.2 in Appendix A). In February the wind speeds in the Skagerrak are weak and westerly winds are prevailing. In March northerly winds are prevailing. Another more clear outflow event occurs at the beginning of March. Now bigger and more distinct eddies than after the event of January are clearly visible in Figure 6.2 and start to propagate northwards. A zoomed view of the temperature and salinity plots in Figure 6.3, plotted together with velocity vectors clearly shows that the surface currents follow the patterns of the sea surface temperature and salinity.

In the months April to September the magnitudes of the wind speed are clearly smaller than in the winter months. In April northerly and southerly winds are found along the coast of Norway. In May clear South-westerlies are prominent north of 63°N and merely easterly along the coast of Norway. In June clear southerly winds are present along the entire coast of Norway, as well as in the Skagerrak. In the following months up to October the main wind direction is from south and south-westerly direction. At the end of November another clear outflow event occurs, again the resulting eddies are visible in the surface salinity and temperature and the structure of the currents along the west coast.

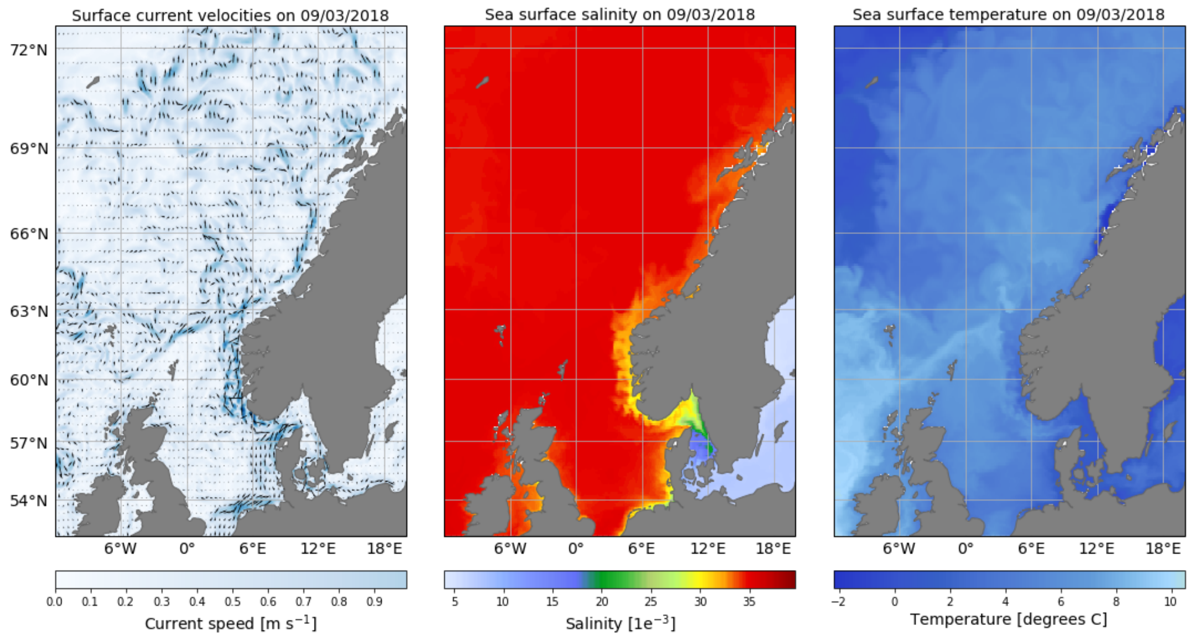

Figure 6.2: Surface currents, sea surface salinity and sea surface temperature for the North Sea and NCC on March 9th 2018

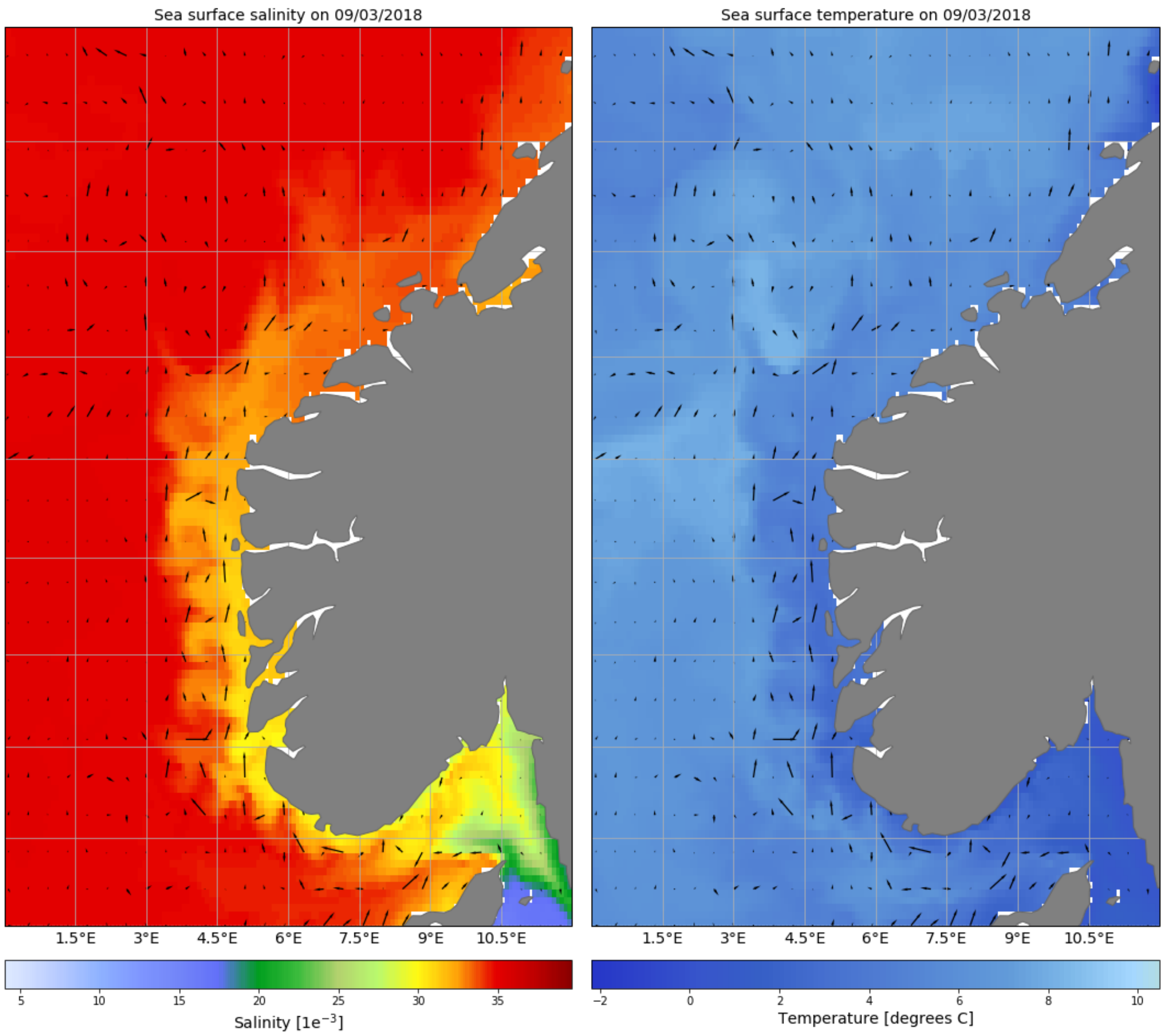

Figure 6.3: Surface currents, sea surface salinity and sea surface temperature for the North Sea and NCC on March 9th 2018

6.2 Particle trajectories for one year

The results of the simulation with a run time of one year, with starting points according to the interest of Van Oord, are shown in Figure 6.4. Starting locations are indicated by a star, scaled to working depths of the works, which is related to the amount of plastics released as explained in Section 1.1. The coloured dots give an indication of the 'age' (in days) of the particle. All particles released south of the Skagerrak circulate in the Skagerrak before reaching the NCC. Particles released along the coast of Norway float northwards in the NCC. The particle released north of Scotland moves in southeast direction and passes between Orkney and mainland Shetland before reaching the NCC. This particle gets stuck along the Norwegian coast (64.25°N, 10.33°E) after day 282. Another particle that gets stuck is the one released just off the Dutch coast, it stays at the same location along the coast of Norway (60.67°N, 5.01°E) after day 305.

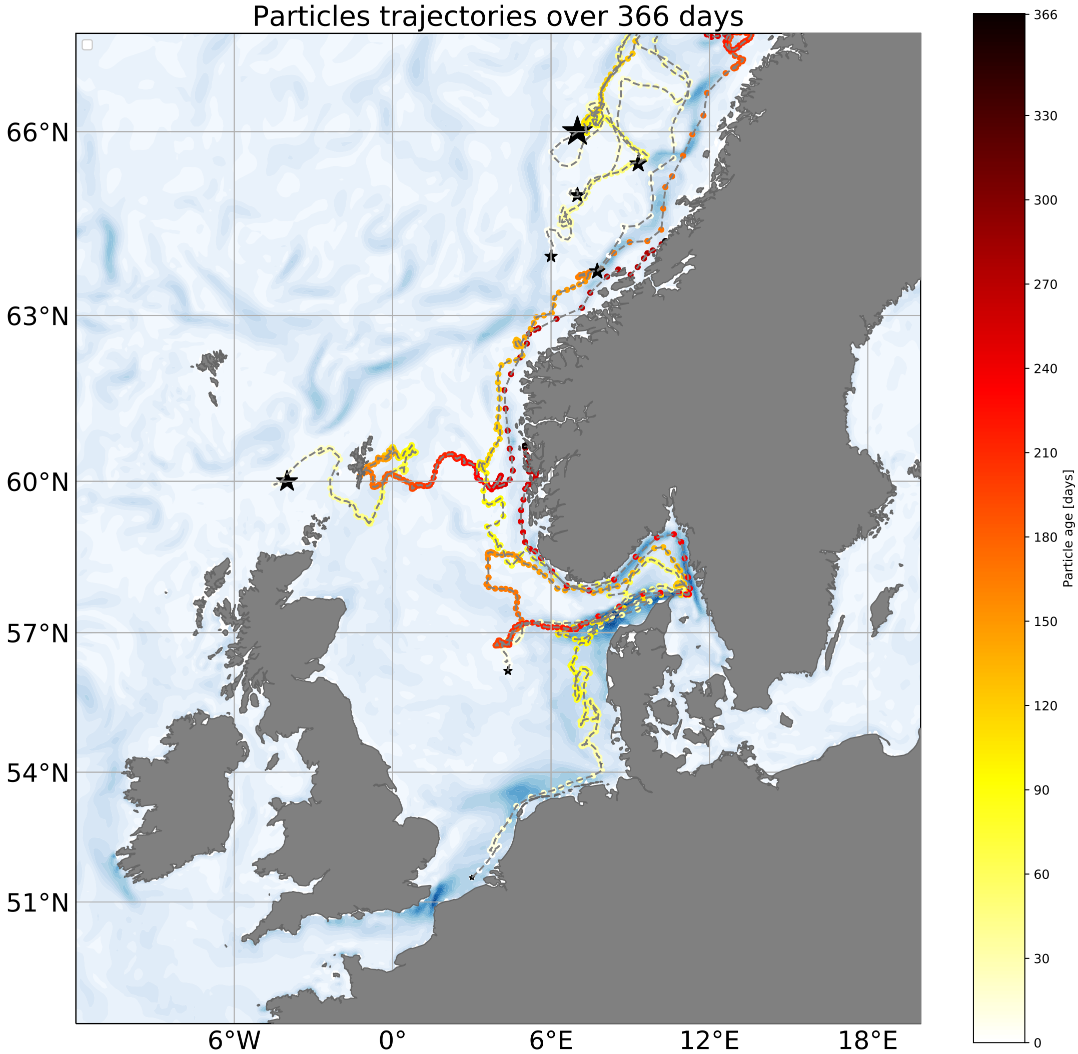

Figure 6.4: Particle trajectories for one year with daily mean input for the surface currents

6.3 Temporal scales

First of all daily-mean values are used as hydrodynamic input for the analysis. According to a rule of thump, the time step for the Lagrangian interpolation is 1/10th of the one of hydrodynamic forcing. This would be 2.4 hours for computations with daily mean inputs, which is in this case rounded to 3 hours. This is the base scenario D180, which is compared to half and double the time step, respectively scenario D90 and D6. An overview of the scenarios is described in Table 6.1.

Scenario	Hydrodynamic forcing	Time step Lagrangian interpolation	Time step output
D180	Daily-mean, $\boldsymbol{vo}$	3 hours	24 hours
D90	Daily-mean, $\boldsymbol{vo}$	1.5 hours	24 hours
D6	Daily-mean, $\boldsymbol{vo}$	6 hours	24 hours
H6	Hourly-mean, $\boldsymbol{vo}$	6 minutes	24 hours
H6vt	Hourly-mean, $\boldsymbol{v}_{total}$	6 minutes	24 hours

Table 6.1: Overview of different scenarios for the temporal scale

Figure 6.5 shows the particle trajectories of 8 particles released at the same locations to the ones of Figure 6.4 for scenarios D180, D90 and D6. The computation is run over a period of 3 months, even though the time steps for the computation differ, the outputs for all scenarios are 24 hours.

Scenarios D180 and D90 with time steps of 3 hours and 1.5 hours respectively, both show the same trajectories (see yellow and pink dots in Figure 6.5). With this computation a time step of 3 hours is validated. A time step of 6 hours would significantly decrease the computation time, hence this is also compared to the trajectories of the smaller time steps. However, as can be seen in Figure 6.5 a computation with a time step of 6 hours (blue squares) has clear deviations from the other two computations. Deviations in meters at the last time step are given in Table 6.2. The particle locations after 90 days with a time step of 6 hours show deviations ranging between 1.2 and 222.6 km, with an average of 51 km compared to the smaller time steps considered. Hence, for a computation with daily mean values for the flow field a time step for the particle tracking of 3 hours is optimum.

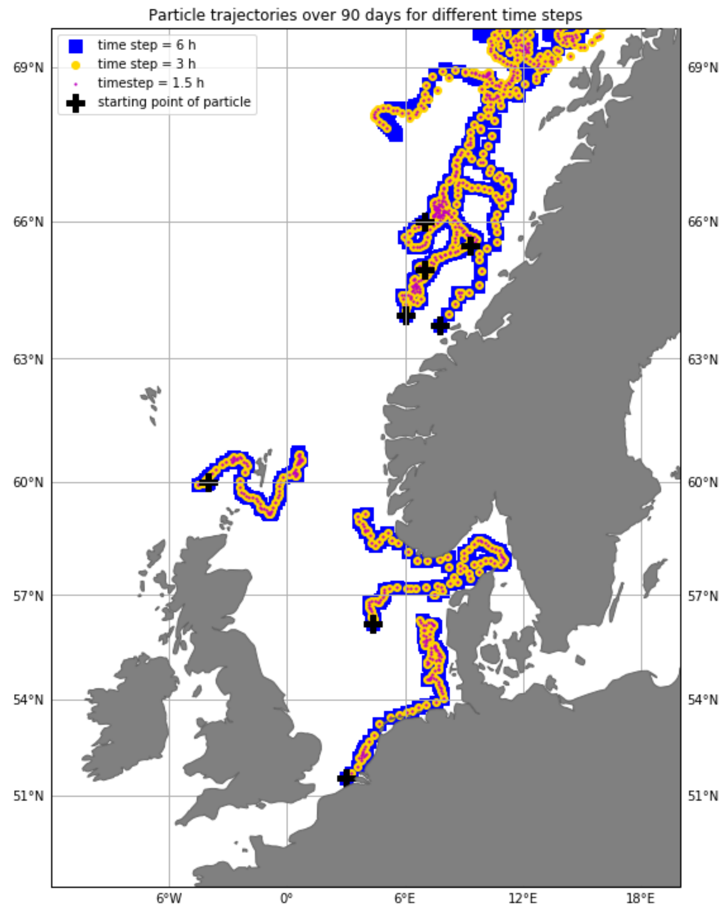

Figure 6.5: Particle trajectories for different time steps for the Lagrangian interpolation, according to scenarios D180 (yellow dots), D90 (pink dots) and D6 (blue squares)

To examine the difference between daily-mean and hourly-mean values again 8 particles are released from the same locations as before. Figure 6.6a shows the difference in particle trajectories for computations with an daily-mean input of the ocean current velocity $\boldsymbol{vo}$ (yellow dots) and hourly-mean input of the ocean current velocity $\boldsymbol{vo}$ (blue dots), scenario D180 and D90 respectively. Computations with hourly mean inputs use a time step of 6 minutes for the particle tracking (and is validated similarly to scenario D180), and computation with daily input uses a time step of 3 hours. However both outputs are the particle locations every 24 hour for both computations. Some deviations can be seen between hourly inputs and daily inputs for the flow field. Those deviations are different, for the different locations of release. Those difference range from 2.2 to 220.7 km, with an average of 45 km for the last time step (after 31 days), with the most deviating trajectories along the coast of Norway.

Figure 6.6b shows trajectories for hourly-mean input for the ocean current ($\boldsymbol{vo}$, yellow dots) and hourly-mean input of the total velocity ($\boldsymbol{v}_{total} = \boldsymbol{vo} + \boldsymbol{v}_{tide} + \boldsymbol{v}_{wave}$, pink crosses). The total velocity is the ocean current velocity with an addition of the tide- and wave-induced currents, according to Equation 6.1. The trajectories are clearly different, for the different locations of release. Those differences range from 42.1 to 344.3 km, with an average of 126 km for the last time step (after 31 days).

$$\boldsymbol{v}_{total} = \boldsymbol{vo} + \boldsymbol{v}_{tide} + \boldsymbol{v}_{wave} \tag{6.1}$$

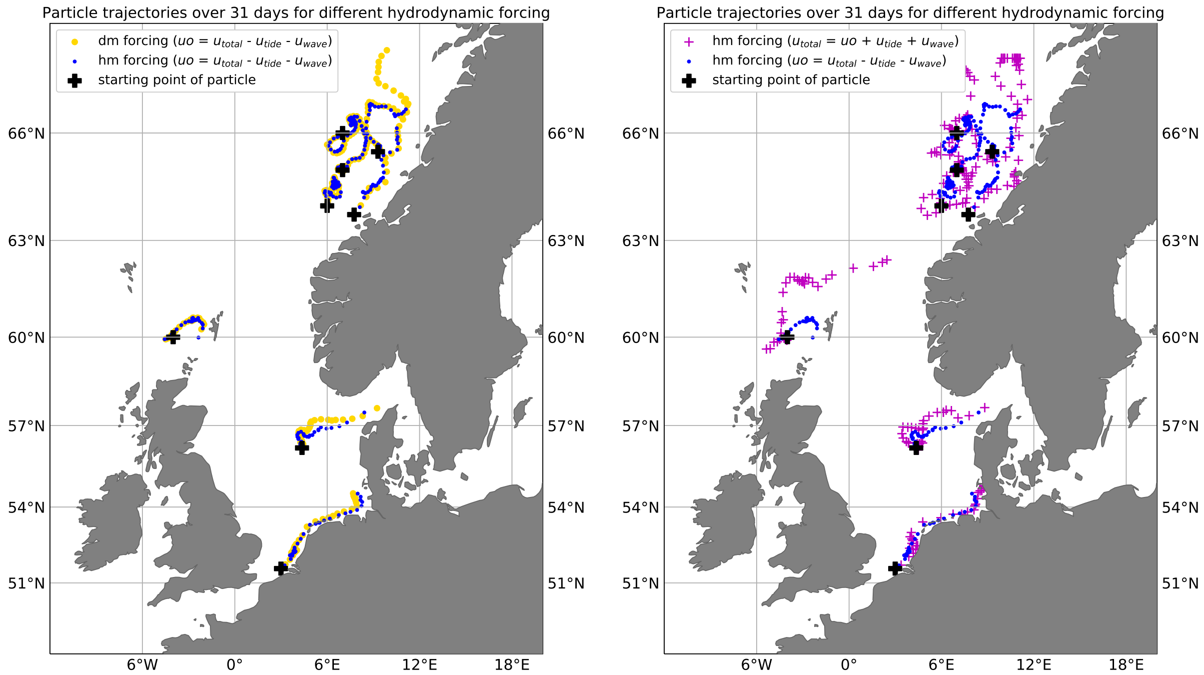

(a) (b)

Figure 6.6: Particle trajectories for different temporal scales and components of the hydrodynamic forcing (a) according to scenarios D180 (yellow dots) and H6 (blue dots) to show the effect of daily vs hourly forcing (b) according to scenarios H6 (blue dots) and H6vt (pink crosses) to show the effect of addition of tides and waves

.

	D180	D90	D6	H6	H6vt
D180		0.0	1.2-222.6 km	2.2-220.7 km	42.1-344.3 km
D90	0.0		1.2-222.6 km	2.2-220.7 km	42.1-344.3 km
D6	1.2-222.6 km	1.2-222.6 km		×	×
H6	2.2-220.7 km	2.2-220.7 km	×		×
H6vt	42.1-344.3 km	42.1-344.3 km	×	×	

Table 6.2: Deviations between the different scenarios for the particle location at the last time step

7 Discussion

The spatial scale of the used model is relatively coarse. The grid size is in the order magnitude of the internal Rossby radius along the Norwegian coast, and bigger than the internal Rossby radius on the North Sea shelf. So in the model the effect of Coriolis on stratified flows is not taken into account for the North Sea shelf. This course model does not take coastal processes into account.

In the particle tracking simulation microplastic particles are assumed to be floating and merely following the surface currents in a 2D plane. Vertical dynamics are therefore fully neglected. However, if the spreading of microplastics is studied in a more general sense with varying plastic densities 3D computations should be considered. A study by Delandmeter and van Sebille (2019) investigated the difference between surface particles and passive particles. Those passive particles can also follow vertical flows in the 3D space. A clear difference was found in trajectories and resulting concentrations: floating particles are more likely to accumulate along the coast and thus a smaller fraction reaches the Arctic. Processes such as wind-induced turbulence, organisms attaching to plastic particles, trapping in settling sediment or trash can lead to plastic distribution over depth (Eriksen et al., 2014)

The boundaries of the domain are set, as such that the particles that want to leave the domain stick at the boundary. This is for practical reasons, otherwise OceanParcels gives an error when a particle leaves. However, this sometimes causes particles to re-enter the domain at an undesired location. Those particles might follow a path that is not realistic. A more realistic boundary condition at the end of the domain would be an open boundary, so that particles can leave the domain. This would imply a change in the particle tracking simulation such that particles that leave the domain will be removed from the computation.

The coastal boundaries are set as impermeable boundaries. In Figure 6.4 can be seen that particles get stuck along the coast. In reality a plastic particle could get trapped along the coast if there is a persistent onshore current and coastal downwelling. However, in the particle trakcing simulation the particles stay in exactly the same location for over 60 days, which make it more likely that the particles got stuck in a dry cell.

In reality the hydrodynamic forcing and the resulting physical particle behaviour determines whether particles will be washed ashore, float along the coast or leave the coastal area again. If the processes which allow for beaching are not included in the particle tracking simulation, the problem can be solved by adding an artificial current pushing a particle back when it has reached a dry cell, as done by Delandmeter and van Sebille (2019).

Particle trajectories of 8 individual particles released from 8 different locations show a lot of difference if there is a variation in the input for the hydrodynamic forcing. Computations with an hourly-mean or daily-mean input of the ocean currents shows a significant divergence for the individual particles. After 31 days the average difference between the pairs of 8 particles is 45 km. Computations with hourly-mean input for just the ocean current and the total velocity (ocean current + tide-induced current + wave-induced current) show even more divergence. After 31 days an average of 126 km is found for the 8 particle pairs.
If a lot of particles are released and the resulting concentrations and spreading would be examined, it might not cause such a significant difference. Especially when hourly-mean and daily mean values are compared, it might average out the differences when a lot of particles have been released.

The qualitative estimate is done for fjords perpendicular to the wind direction, for a narrow fjord. This way a 2D configuration can be assumed. However, various fjords have a more complex shape, which make it hard to say something about the residual flow patterns. In fjords with a complicated shape various 3D flow patterns may arise due to Coriolis.

7.1 Recommendations

In future studies the following aspects could be further examined:

- Investigate whether microplastic particles actually stay afloat.
- Computations with a 3D model for the currents and particle tracking.
- Computations including Stokes drift and/or diffusion, allowing for beaching (Delandmeter and van Sebille, 2019).
- Computations with a finer resolution near the coast and a model that resolves coastal processes. Special attention can be drawn to interaction with the Norwegian fjords. A coarse model could be run to obtain boundary conditions for the coastal model.
- Model the release of numerous particles from the same location to investigate the spatial spreading of particles. From such computations the resulting concentrations can be determined for locations of interest.
- Check stability of the pasrticle tracking simulation and/or logical timescale in relation to spatial scale.
- Check the importance of temporal resolution and input for the hydrodynamic forcing (also including tide-induced and wave-induced currents). Smaller time steps can improve the accuracy of the computation, however it increases the computational time. Hence it should be considered whether a larger temporal resolution gives a valuable better result taking into account the additional computation time.

8 Conclusion

The aim of this study was to answer the following question:

How will microplastics spread in the North Sea after they have been released during offshore operations?

Any plastic particle released in the North Sea eventually gets trapped in the Norwegian Coastal Current (NCC) and gets advected towards the north. From here it is expected that plastic particles will be advected towards the Arctic region or will get trapped in Norwegian fjords. The location of release does not clearly influence where the particle ends up. However, the location of release is important for the time scale for the particle to be advected towards the North.

With daily-mean values for hydrodynamic forcing by only the ocean current velocity the optimum time step for Lagrangian simulation of plastic particle trajectories is 3.0 hours. Comparing this computation to one with hydrodynamic forcing by hourly-mean values of the ocean current velocity (time step of 6 min) shows a deviation. After 31 days differences range between 2.2 and 220.7 km with an average of 45 km for the 8 particle pairs. A computation with hydrodynamic forcing by hourly-mean values of the total velocity (consisting of the ocean current velocity, tide-induced velocity and wave-induced velocity) compared to hourly-mean values of just the ocean current shows a more significant difference after 31 days. Those differences range from 42.1 to 344.3 km, with an average of 126 km.

Data of 2018 of the NCC clearly shows that large scale eddies form along the coast of Norway after a freshwater outflow event from the Skagerrak. Very clear outflow events are observed several times in 2018. After these event, eddies are visible in both the sea surface salinity as well as the sea surface temperature. Also the vectors of the surface currents show eddying patterns. Contrastively, the coastal current is northward directed parallel to the Norwegian coast in other cases. The wind patterns based on monthly-mean values for the wind speed and direction show a seasonal variation in line with literature.

References

Andrady, A. L., & Rajapakse, N. (2019). Additives and chemicals in plastics. In H. Takada & H. K. Karapanagioti (Eds.), *Hazardous chemicals associated with plastics in the marine environment* (pp. 1–17). doi:10.1007/698_2016_124

Barboza, L., Vethaak, A., Lavorante, B., Lundebye, A.-K., & Guilhermino, L. (2018). Marine microplastic debris: An emerging issue for food security, food safety and human health. *Marine Pollution Bulletin*, *133*. doi:10.1016/j.marpolbul.2018.05.047

Beg, M. N. A. (2013). *Implementation of a 3d model for the north sea and uk surrounding area* (MSc Thesis, Brandenburg University of Technology).

Bosboom, J., & Stive, M. (2015). *Coastal Dynamics I* (0.5). Delft Academic Press.

Britannica, E. (n.d.). Norway deep: Submarine trough, north sea. Retrieved October 7, 2019, from https://www.britannica.com/place/Norway-Deep

Cole, M., Lindeque, P., Fileman, E., Halsband, C., Goodhead, R., Moger, J., & Galloway, T. S. (2013). Microplastic ingestion by zooplankton. *Environmental Science & Technology*, *47*(12), 6646–6655. PMID: 23692270. doi:10.1021/es400663f. eprint: https://doi.org/10.1021/es400663f

Copernicus Marine environment monitoring service. (2019). Global ocean 1/12 physics analysis and forecast updated daily. Retrieved October 16, 2019, from http://marine.copernicus.eu/services-portfolio/access-to-products/?option=com_csw&view=details&product_id=GLOBAL_ANALYSIS_FORECAST_PHY_001_024

Delandmeter, P., & van Sebille, E. (2019). The parcels v2.0 lagrangian framework: New field interpolation schemes. *Geoscientific Model Development*, *12*(8), 3571–3584. doi:10.5194/gmd-12-3571-2019

Eriksen, M., Lebreton, L. C. M., Carson, H. S., Thiel, M., Moore, C. J., Borerro, J. C., ... Reisser, J. (2014). Plastic pollution in the world's oceans: More than 5 trillion plastic pieces weighing over 250,000 tons afloat at sea. *PLOS ONE*, *9*, 1–15. doi:10.1371/journal.pone.0111913

Ersdal, G. (2001). An overview of ocean currents with emphasis on currents on the norwegian continental shelf.

Farmer, D. M., & Freeland, H. J. (1983). The physical oceanography of fjords. *Progress in Oceanography*, *12*(2), 147–219. doi:https://doi.org/10.1016/0079-6611(83)90004-6

Gustafsson, B. (1997). Interaction between baltic sea and north sea. *Deutsche Hydrographische Zeitschrift*, *49*. doi:10.1007/BF02764031

Holt, J., & Proctor, R. (2008). The seasonal circulation and volume transport on the northwest european continental shelf: A fine-resolution model study. *Journal of Geophysical Research: Oceans (1978–2012)*, *113*(C6). doi:10.1029/2006JC004034

Inall, M., & Gillibrand, P. (2010). The physics of mid-latitude fjords: A review. *Geological Society of London Special Publications*, *344*, 17–33. doi:10.1144/SP344.3

Klinck, J. M., O'Brien, J. J., & Svendsen, H. (1981). A simple model of fjord and coastal circulation interaction. *Journal of Physical Oceanography*, *11*(12), 1612–1626. doi:10.1175/1520-0485(1981)011⟨1612:ASMOFA⟩2.0.CO;2

Lange, M., & van Sebille, E. (2017). Parcels v0.9: Prototyping a lagrangian ocean analysis framework for the petascale age. *Geoscientific Model Development*, *10*(11), 4175–4186. doi:10.5194/gmd-10-4175-2017

Lebreton, L. C. M., van der Zwet, J., Damsteeg, J.-W., Slat, B., Andrady, A., & Reisser, J. (2017). River plastic emissions to the world's oceans. *Nature Communications*, *8*, 1–15. doi:10.1038/ncomms15611

Maslowski, W., & Walczowski, W. (2002). Circulation of the baltic sea and its connection to the pan-arctic region - a large scale and high-resolution modeling approach.

McClimans, T. A., & Nilsen, J. H. (1983). Whirls in the norwegian coastal current. In H. G. Gade, A. Edwards, & H. Svendsen (Eds.), *Coastal oceanography* (pp. 311–320). doi:10.1007/978-1-4615-6648-9_17

Mork, M. (1981). Circulation phenomena and frontal dynamics of the norwegian coastal current. *Philosophical Transactions of the Royal Society of London. Series A, Mathematical and Physical Sciences*, *302*(1472), 635–647. Retrieved from http://www.jstor.org/stable/37043

NHL Sintef-Gruppen, N. H. L. (n.d.). *Forcasting ocean currents of the northern north sea.* Video, 1984.

NOAA. (2018). What are microplastics? Retrieved June 25, 2018, from https://oceanservice.noaa.gov/facts/microplastics.html

NOS. (2019). Who: Plastic in drinkwater lijkt geen bedreiging, 'maar zorg begrijpelijk'. Retrieved August 22, 2019, from https://nos.nl/artikel/2298464-who-plastic-in-drinkwater-lijkt-geen-bedreiging-maar-zorg-begrijpelijk.html

OceanParcels project. (2019). What is oceanparcels? Retrieved October 16, 2019, from http://oceanparcels.org/

OffshoreEngineering.com. (n.d.). Ekman current, upwelling, downwelling. Retrieved October 14, 2019, from https://www.offshoreengineering.com/education/oceanography/ekman-current-upwelling-downwelling

OSPAR. (2000). Quality status report 2000 region II — Greater North Sea. *OSPAR Commission London*. 136 pp.

Pietrzak, J. D. (2018a). *An introduction to oceanography for civil and offshore engineers.* Delft: Delft University of Technology.

Pietrzak, J. D. (2018b). *An introduction to stratified flows in civil and offshore engineers.* Delft: Delft University of Technology.

Pot, H. (2019). *Measurements on micro plastic loss due to subsea rock installation.* Technical Report - Van Oord Dredging and Marine Contractors bv.

Skagseth, Ø., Slotte, A., Stenevik, E. K., & Nash, R. D. (2015). Characteristics of the norwegian coastal current during years with high recruitment of norwegian spring spawning herring (clupea harengus l.) *PubMed*, *10*. Retrieved from https://www.ncbi.nlm.nih.gov/pubmed/26636759

Stigebrandt, A. (2012). Hydrodynamics and circulation of fjords. In L. Bengtsson, R. W. Herschy, & R. W. Fairbridge (Eds.), *Encyclopedia of lakes and reservoirs* (pp. 327–344). doi:10.1007/978-1-4020-4410-6_247

Tande, K. (2001). Fiordic ecosystems. In *Encyclopedia of ocean sciences (second edition)* (pp. 359–366). Academic Press. Retrieved from https://doi.org/10.1016/B978-012374473-9.00092-8

Van Oord. (2019a). Subsea Rock Installation (SRI). Retrieved September 16, 2019, from https://www.vanoord.com/subsea-rock-installation-sri

Van Oord. (2019b). Sustainable Earth Actions (S.E.A.) Retrieved September 18, 2019, from https://www.vanoord.com/sustainability/about-programme

van Miltenburg, E. (2017). *Spreading of polluted sediment around the u-864 wreck* (Master's thesis, Delft University of Technology).

Winther, N. G., & Johannessen, J. A. (2006). North sea circulation: Atlantic inflow and its destination. *Journal of Geophysical Research: Oceans*, *111*(C12). doi:10.1029/2005JC003310. eprint: https://agupubs.onlinelibrary.wiley.com/doi/pdf/10.1029/2005JC003310

A Additional figures

A.1 Surface currents, sea water salinity and temperature

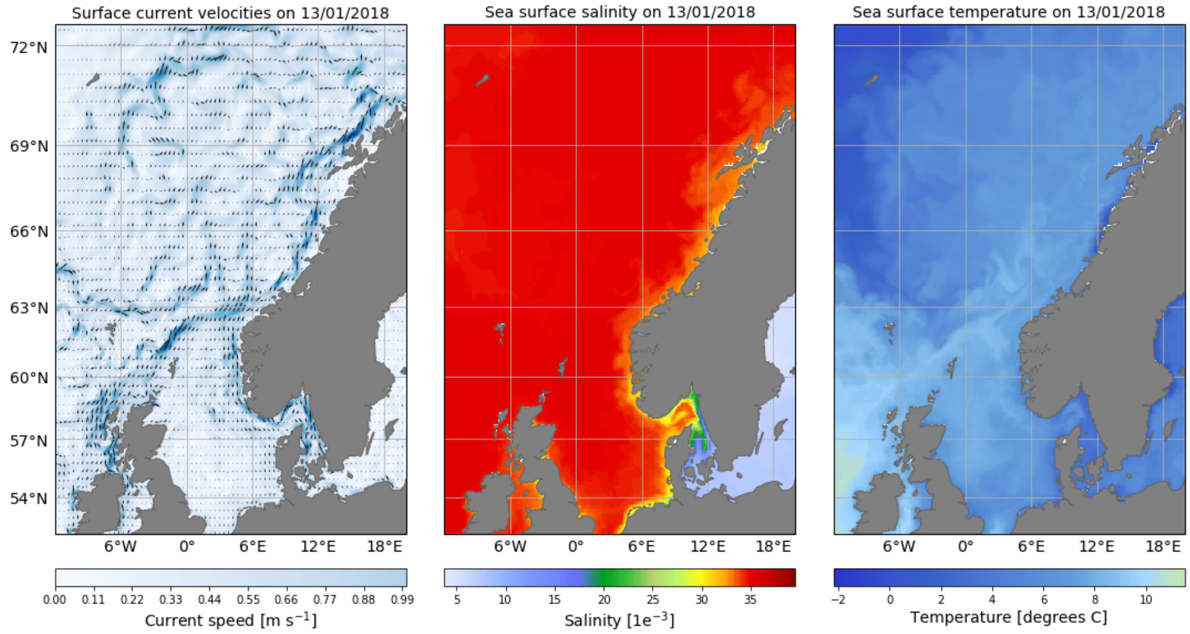

Figure A.1: Surface currents, sea surface salinity and sea surface temperature for the North Sea and NCC on January 13th 2018, showing and outflow event of the Skagerrak

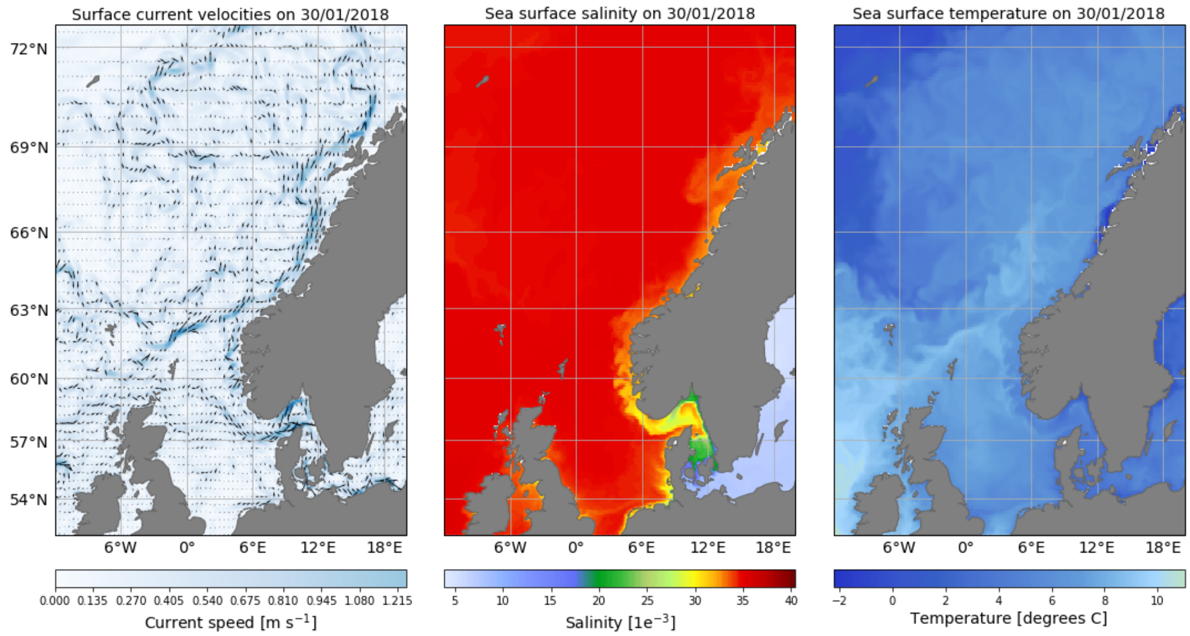

Figure A.2: Surface currents, sea surface salinity and sea surface temperature for the North Sea and NCC on January 30th 2018, showing large scale eddies off the coast of Norway

A.2 Wind patterns

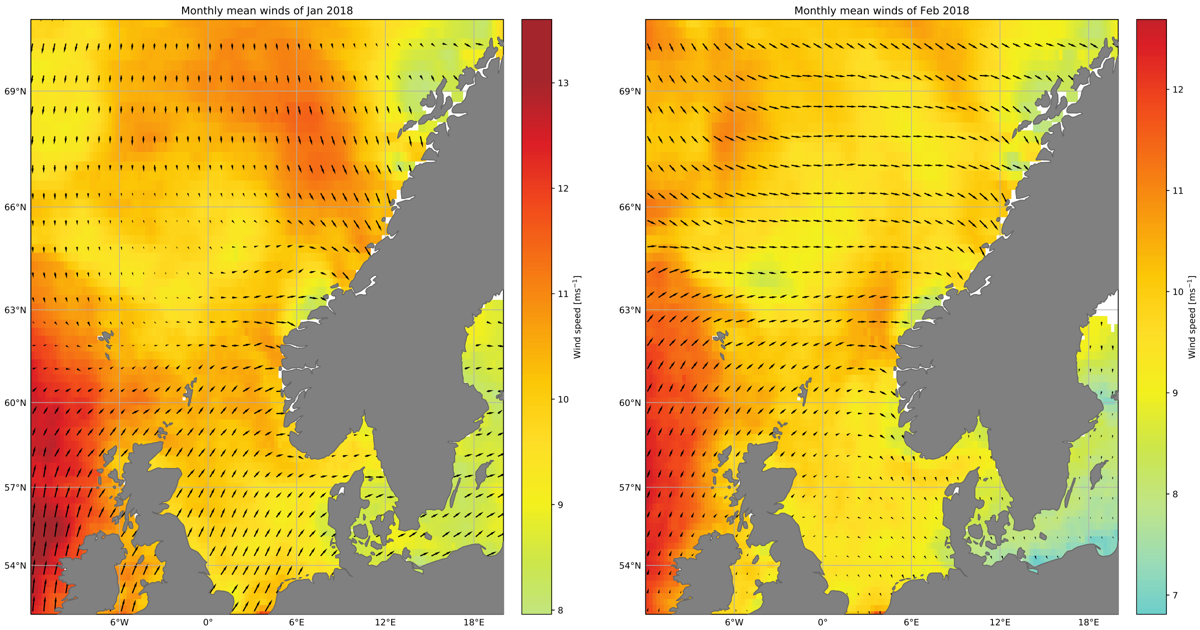

(a) (b)

Figure A.3: Monthly mean wind magnitude and direction (a) January 2018 (b) February 2018

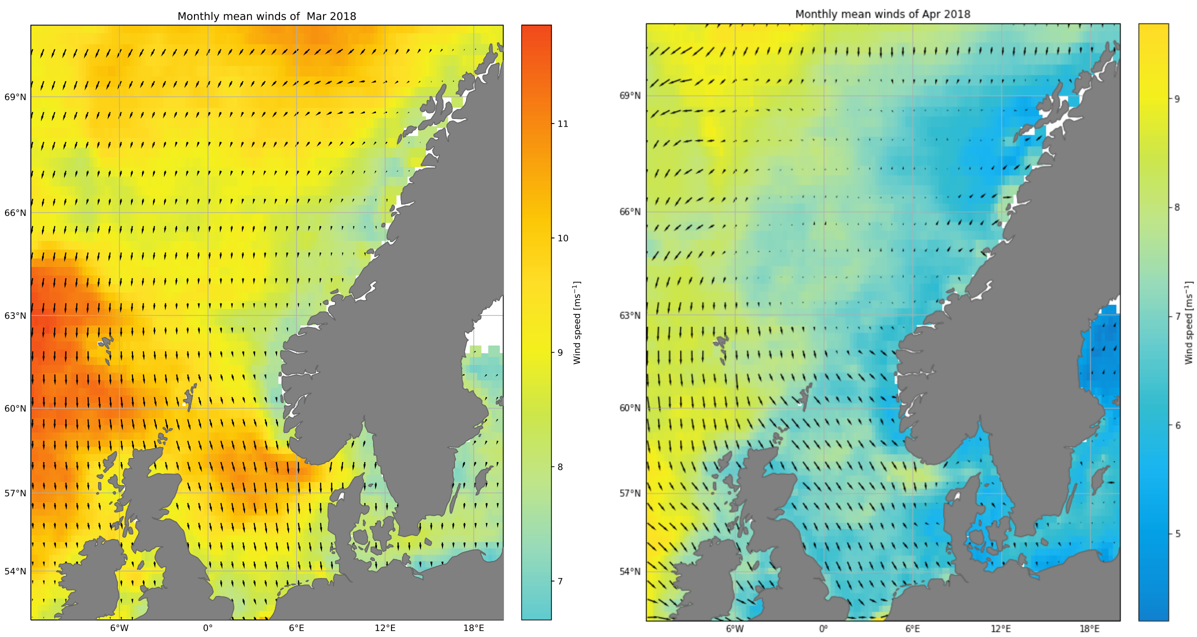

(a) (b)

Figure A.4: Monthly mean wind magnitude and direction (a) March 2018 (b) April 2018

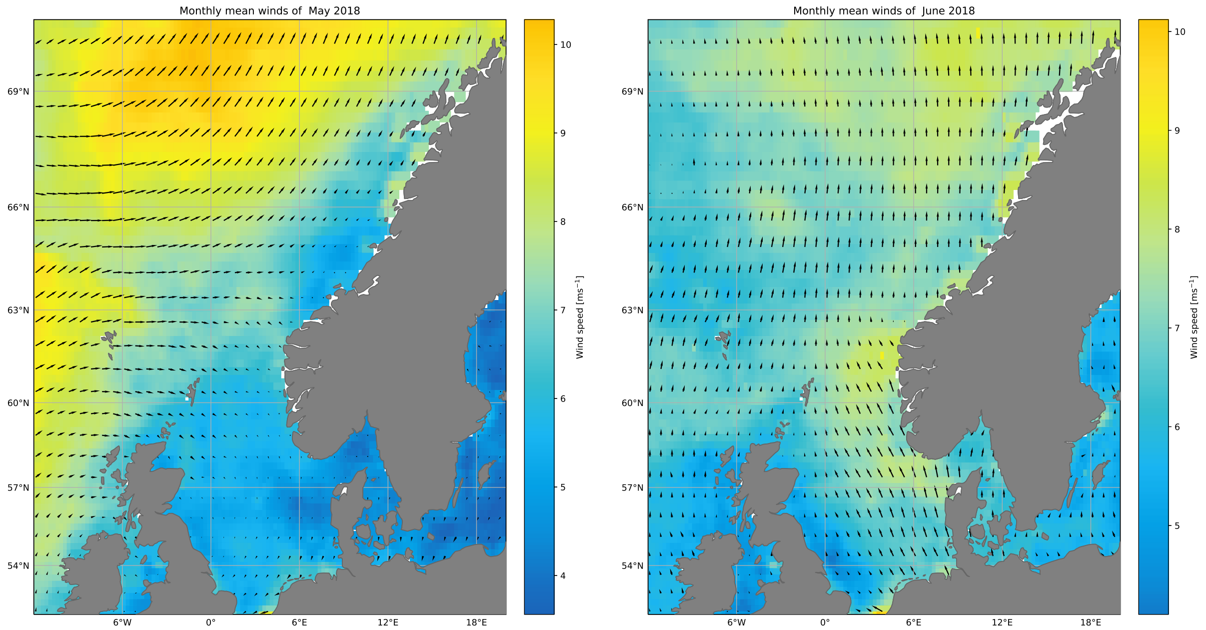

(a) (b)

Figure A.5: Monthly mean wind magnitude and direction (a) May 2018 (b) June 2018

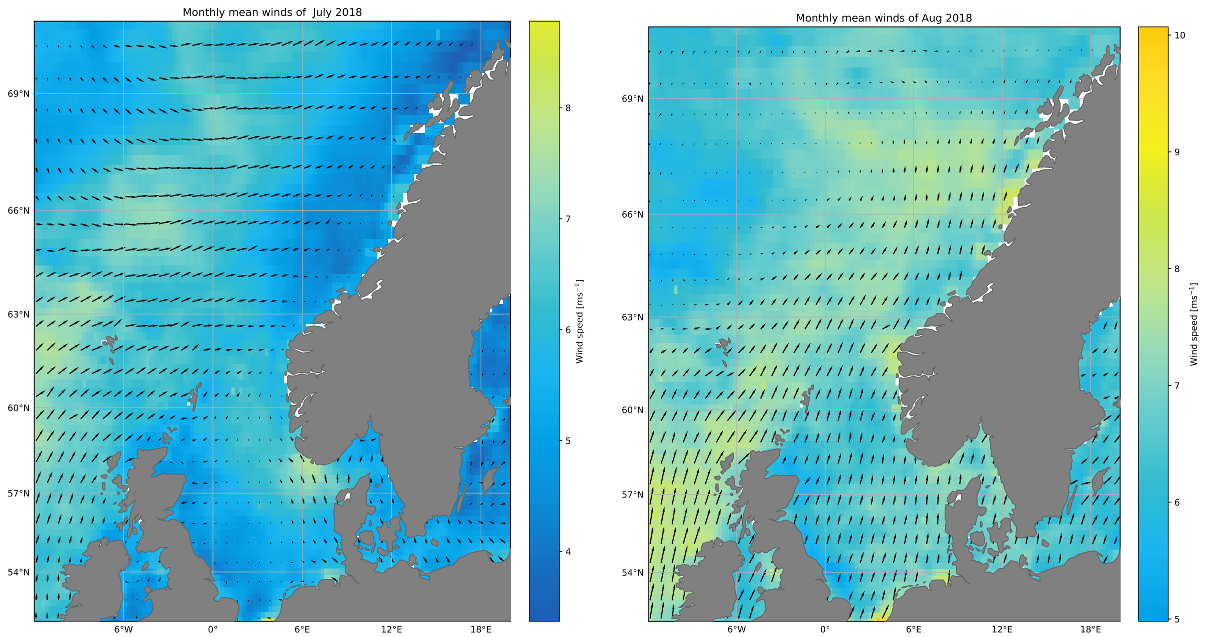

(a) (b)

Figure A.6: Monthly mean wind magnitude and direction (a) July 2018 (b) August 2018

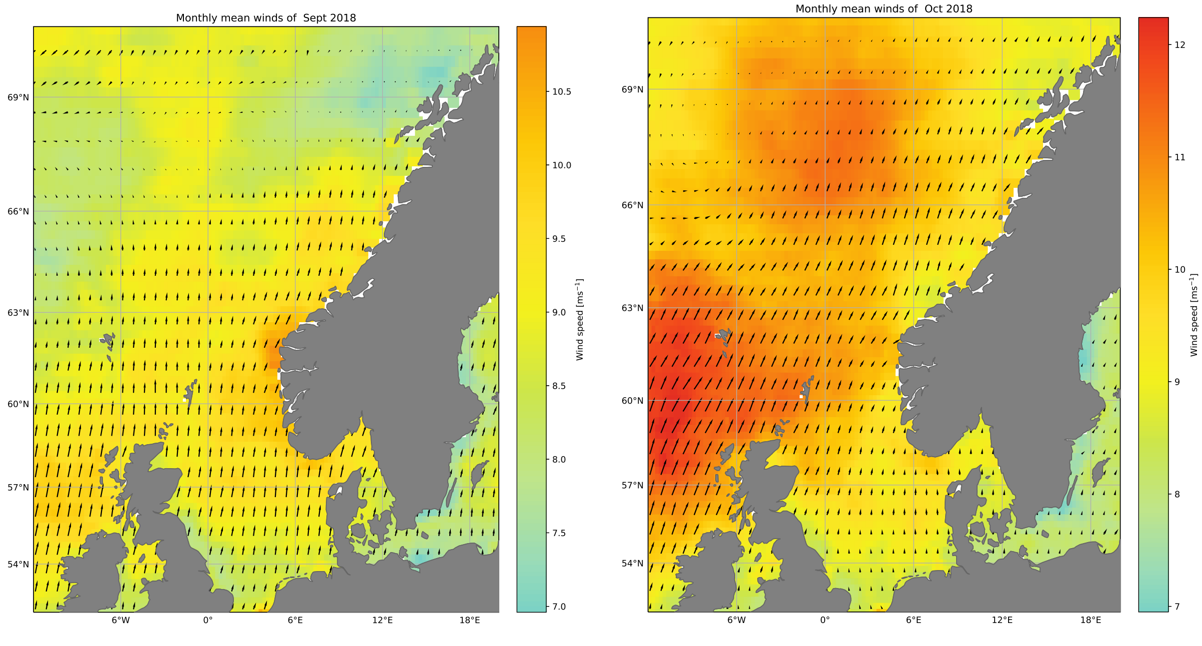

(a) (b)

Figure A.7: Monthly mean wind magnitude and direction (a) September 2018 (b) October 2018

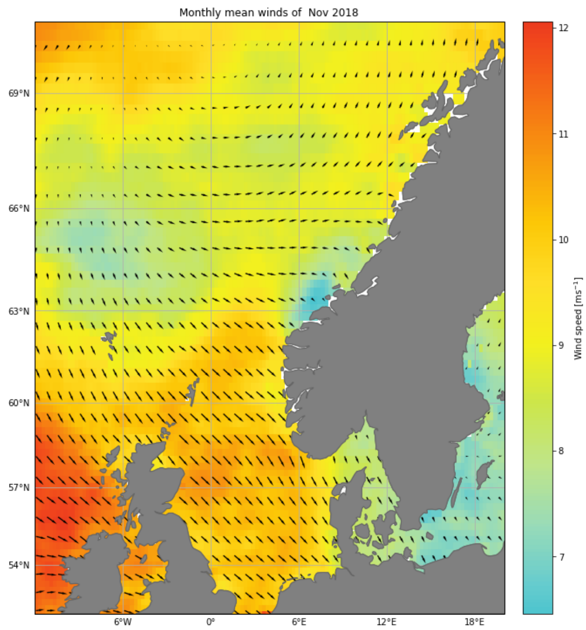

Figure A.8: Monthly mean wind magnitude and direction November 2018